A New Frequency Domain Filter for Precise Phasor Computation of Electrical Power Current

Doaa Khalil IBRAHIM
Electrical Power and Machines Department, Faculty of Engineering, Cairo University, Egypt

Mohamed Essam REZK
Egyptian Electricity Transmission Company EETC, Egypt

Abstract**:** *Digital filters of electrical protective relays play primary roles in calculating the fundamental phasors of electrical power signals. In most fault cases, large amounts of decaying DC components are included in the current signals during the fault period. Decaying DC component significantly reduces the precision and convergence speed of all conventional frequency-domain filters such as Fourier and Walsh filters. In this investigation, this paper introduces a new frequency-domain filtering algorithm to remove the decaying DC components and accurately capture the fundamental power system phasors for digital protective relays. This is executed by means of a mathematical procedure using digital signal processing techniques. The proposed filter is tested for a wide variety of current signals during different fault conditions to assess its performance. The simulation results show that the proposed filtering algorithm has a superior performance at a wide range of decaying components.*

Key words*: Digital filters, Discrete time signal, Decaying DC component, Filtering algorithms, Phasor estimation*.

1. Introduction

The majority of fault current signals have large amounts of decaying DC components. These components have sets of non-integer harmonics [1]. As a result, the decaying DC components of the current signal adversely affect the precision and convergent speed of most conventional filtering algorithms such as discrete Fourier transform (DFT), Kalman filter, Walsh filter, cosine filter, and least-squares-fitting [2].

Many efforts have been exerted to eliminate the negative effect of decaying DC component and improve the performance of the numerical protective relays under the presence of this component. Fixed full cycle DFT (FCDFT) based algorithm has been suggested in [3]. This algorithm uses three continuous FCDFT phasors shifted by one sample to remove the decaying DC component from the signal and obtain the fundamental frequency phasor. In [4], another technique for removing the exponential component has been proposed based on calculating the unknown parameters of the decaying DC component using a simple mathematical formula. Then, the fundamental phasor is calculated by FCDFT after subtracting the computed decaying DC component from the original signal. A method based on the integration of the fault current during one power cycle has been proposed in [5]. This method uses the integration process to determine the magnitude and time constant of the decaying DC offset. Then, the decaying component is removed by subtracting the DC offset value from the signal at each sampling instant. A method based on even and odd sample set DFT has been proposed in [6]. The phasor corresponding to the decaying DC component is estimated by using odd and even sample set DFT phasor, and then this phasor is subtracted from the original DFT phasor to obtain the fundamental phasor. In [7], a method to eliminate the effect of decaying DC component using two FCDFT phasors shifted by half cycle has been proposed. In [8], a method based on combined full and half cycle Fourier algorithms has been proposed for quickly removing the decaying DC component and estimating the fundamental frequency phasors.

Generally, the effect of the decaying DC components can be solved using two main approaches. The first approach is based on making some modifications in the conventional frequency domain filters, while the second one is depending on building a new frequency domain filter which immune to the decaying components. All the aforementioned techniques proposed in [3-7], are based on the first approach. However, using the frequency-domain filters in fundamental phasors estimation can give more secure operation of the protective relays as the performance of such filters at all frequencies is well defined according to their frequency response so that the second approach is applied in this paper for removing the decaying components.

A new effective frequency-domain filter, using only one and quarter cycle data window, is proposed for filtering fault currents. The proposed filtering technique is based on multiplying each power cycle of the current input signal by particular functions. These functions are fully defined in the period of one power cycle. The frequency response of the proposed filter and its performance for different levels of decaying DC component are extensively discussed.

2. Proposed Filter Algorithm

To discuss the technique used by the proposed

BUPT

filter in filtering out the DC component and integer harmonics, consider that the continuous signal x (t) contains DC component (A_0), fundamental frequency component, even harmonics, and a set of odd harmonics of $(10r-5)^{th}$order.

It is notable that this signal is only used to describe the proposed filter, while the performance of proposed filter for the remaining odd harmonics is fully implemented in the next section. The signal x (t) can be expressed as follows:

$$x(t) = A_0 + A_1\sin(\omega t + \Phi_1) + \sum_{r=1}^{h} A_{2r}\sin(2r\omega t + \Phi_{2r}) + \sum_{r=1}^{h} A_{(10r-5)}\sin[(10r-5)\omega t + \Phi_{(10r-5)}] \quad (1)$$

Where A_1 and Φ_1 are the magnitude and phase angle of the fundamental component. $\omega = \frac{2\pi}{T}$ is the fundamental angular frequency of a period T. A_{2r} and Φ_{2r} are the magnitude and phase angle of the $2r^{th}$ order harmonic component, respectively. Also, $A_{(10r-5)}$ and $\Phi_{(10r-5)}$ are the magnitude and phase angle of the $(10r-5)^{th}$ order harmonic component, respectively, where h is the maximum harmonic order.

The fundamental frequency phasor can be calculated in imaginary and real parts Xi, Xr respectively.

For finding the value of Xi, the above equation is integrated at different intervals as follows:

$$\text{Let } F1 = \int_0^{T/4} x(t)dt - \int_{T/4}^{13T/20} x(t)dt + \int_{17T/20}^{T} x(t)dt + \int_0^{3T/20} x(t)dt - \int_{7T/20}^{3T/4} x(t)dt + \int_{3T/4}^{T} x(t)dt + \int_0^{T/5} x(t)dt - \int_{\frac{2T}{5}}^{\frac{3T}{5}} x(t)dt + \int_{4T/5}^{T} x(t)dt + \int_0^{T/10} x(t)dt - \int_{3T/10}^{7T/10} x(t)dt + \int_{9T/10}^{T} x(t)dt \quad (2)$$

By using the achieved results demonstrated in Appendix A, it yields:

$$F1 = M \times A_1 \sin(\Phi_1)$$

$$\text{Where } M = \frac{4[1+\sin(54^0)+\sin(72^0)+\sin(36^0)]}{\omega}.$$

$$\text{Thus, } Xi = \frac{1}{M}F1 \quad (3)$$

For finding the value of Xr, the signal x(t) is shifted by quarter cycle and then integrated at the same integration intervals of Equation (2).

$$\text{Let } F2 = \int_0^{T/4} x\left(t+\frac{T}{4}\right)dt - \int_{T/4}^{13T/20} x\left(t+\frac{T}{4}\right)dt + \int_{17T/20}^{T} x\left(t+\frac{T}{4}\right)dt + \int_0^{3T/20} x\left(t+\frac{T}{4}\right)dt - \int_{7T/20}^{3T/4} x\left(t+\frac{T}{4}\right)dt + \int_{3T/4}^{T} x\left(t+\frac{T}{4}\right)dt + \int_0^{T/5} x\left(t+\frac{T}{4}\right)dt - \int_{2T/5}^{3T/5} x\left(t+\frac{T}{4}\right)dt + \int_{4T/5}^{T} x\left(t+\frac{T}{4}\right)dt + \int_0^{T/10} x\left(t+\frac{T}{4}\right)dt - \int_{3T/10}^{7T/10} x\left(t+\frac{T}{4}\right)dt + \int_{9T/10}^{T} x\left(t+\frac{T}{4}\right)dt \quad (4)$$

The same previous procedures are applied for determining the value of F2. Therefore,

$$F2 = M \times A_1 \sin(\Phi_1 + \frac{T}{4}) = M \times A_1 \cos(\Phi_1)$$

$$\text{Thus, } Xr = \frac{1}{M}F2 \quad (5)$$

2.1 Proposed Filter in a Continuous Form

For simplifying the Equations (2) and (4), four predefined functions (R1 (t), R2 (t), R3 (t), and R4 (t)) are used in the calculation process. Fig. 1 depicts these four square functions R in a continuous domain, they have values of -1, 0, or +1 during the time interval between t=0 and t=T. Using these functions, the Equations (2) and (4) can be written as follows:

$$F1=\int_0^T [x(t)\times R1(t)]dt+\int_0^T [x(t)\times R2(t)]dt+\int_0^T [x(t)\times R3(t)]dt+\int_0^T [x(t)\times R4(t)]dt \quad (6)$$

$$F2=\int_0^T \left[x\left(t+\frac{T}{4}\right)\times R1(t)\right]dt+\int_0^T \left[x\left(t+\frac{T}{4}\right)\times R2(t)\right]dt+\int_0^T \left[x\left(t+\frac{T}{4}\right)\times R3(t)\right]dt+\int_0^T \left[x\left(t+\frac{T}{4}\right)\times R4(t)\right]dt \quad (7)$$

Hence, for continues signal x(t), the fundamental phasor at time (t1) can be calculated as follows:

$$Xi(t1) = \frac{1}{M}\left[\int_{t1}^{T+t1}[x(t)\times R1(t-t1)]dt + \int_{t1}^{T+t1}[x(t)\times R2(t-t1)]dt + \int_{t1}^{T+t1}[x(t)\times R3(t-t1)]dt + \int_{t1}^{T+t1}[x(t)\times R4(t-t1)]dt\right] \quad (8)$$

$$Xr(t1) = Xi(t1 + \frac{T}{4}) \quad (9)$$

$$A_1=\sqrt{(Xr)^2+(Xi)^2} \quad (10)$$

$$\Phi_1 = arctan\frac{Xi}{Xr} \quad (11)$$

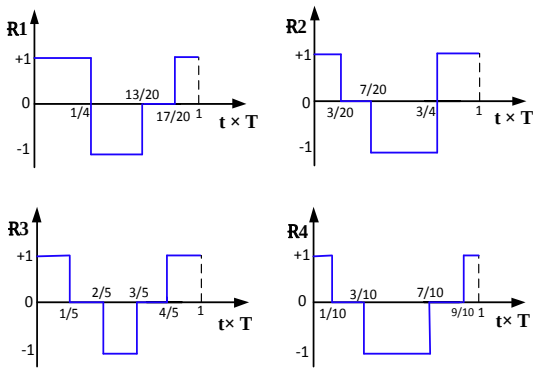


Fig. 1 The four R functions in a continuous domain

BUPT

2.2 Proposed Filter in a Discrete Form

The continuous integral of Equation (8) is not directly adequate for digital processing application. Therefore, the input signal x(t) is sampled at N samples per system cycle, and the n^{th} sample signal x(n) is represented in the following equation:

$$x(n) = A_0 + A_1\sin\left(\frac{2\pi n}{N} + \Phi_1\right) + \sum_{r=1}^{h} A_{2r}\sin\left(2r\frac{2\pi n}{N} + \Phi_{2r}\right) + \sum_{r=1}^{h} A_{(10r-5)}\sin\left[(10r-5)\frac{2\pi n}{N} + \Phi_{(10r-5)}\right] \quad (12)$$

For a discrete signal x(n), the q^{th} sample fundamental phasor can be calculated by converting the Equations (8) and (9) into discrete formula as follows:

$$Xi(q) = \frac{1}{M_d}\left[\sum_{n=q}^{N+q} x(n)\times R1(n-q) + \sum_{n=q}^{N+q} x(n)\times R2(n-q) + \sum_{n=q}^{N+q} x(n)\times R3(n-q) + \sum_{n=q}^{N+q} x(n)\times R4(n-q)\right] \quad (13)$$

$$Xr(q) = Xi\left(q + \frac{N}{4}\right) \quad (14)$$

Where M_d is a discrete formula of M and can be given by: $M_d = \frac{4N[1+\sin(54^0)+\sin(72^0)+\sin(36^0)]}{2\pi}$ (15)

3. Proposed Filter Features

As discussed in the previous derivation, the proposed filter can completely remove all even harmonics, DC component, odd harmonics of $(10r-5)^{th}$ order (r=1, 2, 3, etc.), and can estimate the fundamental phasor. To verify the effectiveness of the proposed filter in removing the remaining odd harmonics, an input signal y1(t) which contains r^{th}order harmonic is applied to the proposed filter as follows:

$$y1(t) = A_r\sin(r\omega t + \Phi_r) \quad (16)$$

For r =3 (3^{rd} harmonic), the proposed filter output can be determined using Equations (8) and (9) as follows:

$$Xi(t1) = \frac{1}{M}\left[\int_{t1}^{T+t1}[y1(t)\times R1(t-t1)]dt + \int_{t1}^{T+t1}[y1(t)\times R2(t-t1)]dt + \int_{t1}^{T+t1}[y1(t)\times R3(t-t1)]dt + \int_{t1}^{T+t1}[y1(t)\times R4(t-t1)]dt\right] \quad (17)$$

After some mathematical manipulations, the values of Xi and Xr at any value of (t1) are deduced by:

$$Xi = \frac{[-1+\sin(18^0)+\sin(72^0)-\sin(36^0)]}{3[1+\sin(54^0)+\sin(72^0)+\sin(36^0)]}\times A_3\sin(3\omega t1+\Phi_3)$$

Also,

$$Xr = \frac{[-1+\sin(18^0)+\sin(72^0)-\sin(36^0)]}{3[1+\sin(54^0)+\sin(72^0)+\sin(36^0)]}\times A_3\cos(3\omega t1+\Phi_3)$$

Thus, the filter output=$\sqrt{(Xr)^2+(Xi)^2}$ = 0.032 A_3

Hence, the proposed filter can remove 96.8% of the magnitude of 3^{rd} harmonic component. The same aforementioned procedure is applied to get the output of the proposed filter for different odd harmonics; the achieved results have been summarized in Table 1.

In real implemented digital protective relays, the input signals are passed through a low pass anti-aliasing filter. This filter is an essential element for all digital relaying algorithms, which eliminates the high frequency oscillations in the signals and prevents aliasing phenomena. The cut off frequency of the low pass anti-aliasing filter is chosen according to Nyquist criterion to be equal or less than half the sampling frequency [9]. For example, the sampling frequency of the modern Siemens digital protective relays is 1 kHz (20 samples per 50-Hz cycle) [10], and the cut off frequency of the low-pass filter should be less than or equal to half the sampling frequency, 500 Hz (10 × fundamental frequency) to prevent aliasing. In other words, this low pass anti-aliasing filter can remove all harmonics greater than the 10^{th}harmonic. Considering this situation, it is sufficient to focus on the harmonics orders less than 10 while the high-frequency components can be easily filtered out by the low pass anti-aliasing filter. However, the behaviour of the proposed filter for higher order harmonics is implemented to provide a clear view of its performance. As clearly deduced from Table 1, the proposed filter has acceptable rejection capability for odd harmonics, as its worst behaviour is achieved for the 19th harmonic with only 94.8% rejection capability.

Fig. 2 depicts the frequency response of the proposed filter; the proposed filter has an appropriate frequency response in those frequencies that exceed twice the fundamental frequency. Besides, the proposed filter exhibits excellent performance in the sub harmonics frequency interval (0 < harmonic order <1) as it has low gain values in this frequency interval. As the decaying DC component is a non-periodic signal whose frequency spectrum includes a wide range of frequencies concentrated in the sub-harmonics frequency interval [9], the proposed filter presents a high level of rejection capability of the exponentially decaying DC component and sub-harmonics as shown in Fig. 2. Moreover a mathematical proof is presented in Section 4 to ensure the robustness of the proposed filter under decaying components of the current signals.

BUPT

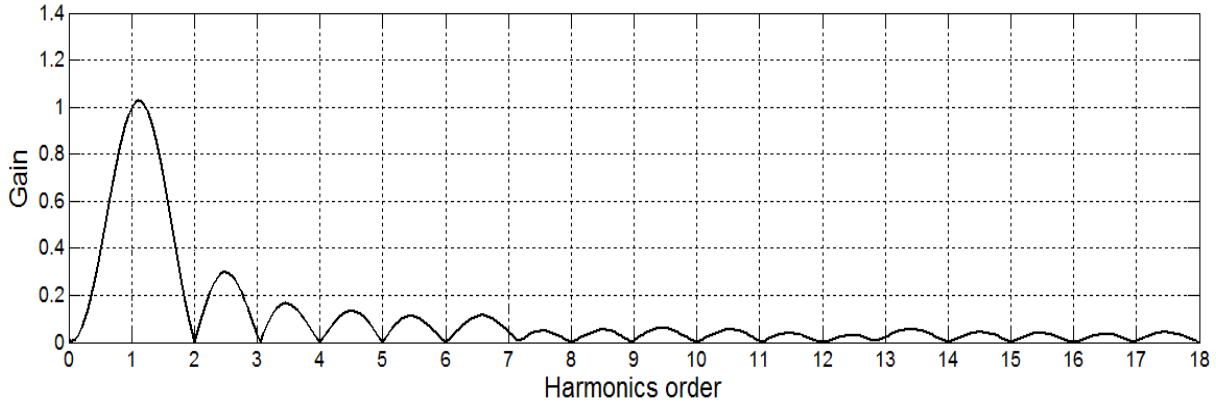


Fig. 2 Frequency response of proposed filter compared with different filtering algorithm

Table 1
Behaviour of proposed filter for odd harmonics removal

Harmonic order	Filter output	Harmonic order	Filter output
r =3	0.032 A_3	r =21	0.046 A_{21}
r =5	0	r =23	0.004 A_{23}
r =7	0.042 A_7	r =25	0
r =9	0.009 A_9	r =27	0.01 A_{27}
r =11	0.008 A_{11}	r =29	0.003 A_{29}
r =13	0.023 A_{13}	r =31	0.002 A_{31}
r =15	0	r =33	0.01 A_{33}
r =17	0.005 A_{17}	r =35	0
r =19	0.052 A_{19}	r =37	0.003 A_{37}

4. Mathematical analysis for estimating the effect of decaying dc component on proposed filter

The decaying DC component is the major component which distorts the fault current signals, while the higher order harmonics seriously distort the fault voltage signals [11].

The input signal y2(t) is used to study the performance of the proposed filter under the influence of exponentially decaying DC signal.

$$y2(t) = I_m e^{\frac{-t}{\tau}} \tag{18}$$

Where I_m and τ are the magnitude and time constant of decaying DC component respectively.

The real and imaginary components Xr_p and Xi_p at time $t1$ can be obtained after applying the proposed filter to $y2(t)$ as follows:

$$Xi_p(t1) = \frac{1}{M}\Big[\int_{t1}^{T+t1}[y2(t) \times R1(t-t1)]dt + \int_{t1}^{T+t1}[y2(t) \times R2(t-t1)]dt + \int_{t1}^{T+t1}[y2(t) \times R3(t-t1)]dt + \int_{t1}^{T+t1}[y2(t) \times R4(t-t1)]dt\Big] \tag{19}$$

$$Xr_p(t1) = Xi_p(t1 + \frac{T}{4}) \tag{20}$$

After some algebraic manipulations, the values of Xi_p and Xr_p at any value of $(t1)$ are given by:

$$Xi_P(t1) = \frac{\tau \times I_m}{M} \times D \tag{21}$$

$$Xr_P(t1) = \frac{\tau \times I_m}{M} \times D \times B^{T/4} \tag{22}$$

Where: $B = e^{\frac{-1}{\tau}}$ and

$$D = 4B^{t1} - 2B^{\frac{T}{4}+t1} + B^{\frac{13T}{20}+t1} + B^{\frac{17T}{20}+t1} - 4B^{T+t1} - B^{\frac{3T}{20}+t1} + 2B^{\frac{3T}{4}+t1} - B^{\frac{7T}{20}+t1} - B^{\frac{T}{5}+t1} + B^{\frac{3T}{5}+t1} - B^{\frac{2T}{5}+t1} + B^{\frac{4T}{5}+t1} - B^{\frac{T}{10}+t1} + B^{\frac{7T}{10}+t1} - B^{\frac{3T}{10}+t1} + B^{\frac{9T}{10}+t1} \tag{23}$$

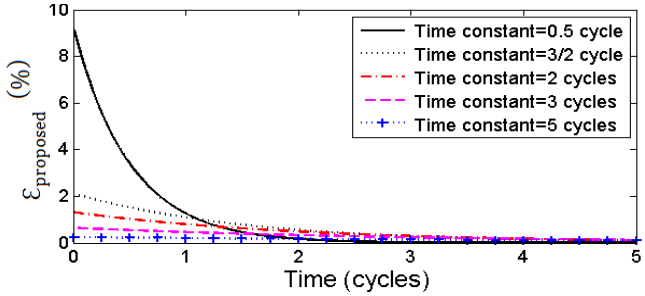


Fig. 3 Performance of the proposed filter for different time constants

The percentage ratio between the magnitude of the output proposed filter and the magnitude of decaying DC component at time t1 can be observed from:

$$\varepsilon_{proposed}(t1) = \frac{\sqrt{\left(Xr_p(t1)\right)^2 + \left(Xi_p(t1)\right)^2}}{I_m} \times 100\ \% \tag{24}$$

This equation describes the performance of the proposed filter for different time constants as illustrated in Fig. 3. For most of the power transmission systems, the variation of time constant value (τ) can be limited in definite boundaries, such as one-half to five cycles [12], which are selected in this study. As shown from Figure 3, the proposed filter can provide appropriate rejection capability of the exponentially decaying DC components for all time constants. Moreover, all peak error values of

BUPT

the proposed filter can be neglected for all time constant values that are greater than or equal to one power cycle.

5. Simulation Results

In order to verify the effectiveness of the proposed filtering algorithm, the proposed filtering technique is evaluated using different test current signals and a simulated power system. The sampling frequency is taken by 12 kHz (240 samples per cycle for 50 Hz system).

5.1 Performance Analysis using Test Signals

In order to adequately demonstrate the performance of the proposed algorithm, some test cases using customized waveforms are examined first.

Case I: Test signals with varied time constants

The MATLAB software program is used to generate three different test current signals as follows:

- $I_1(t)=100\sin(2\pi 50t) - 100e^{\frac{-t}{0.02}}$
- $I_2(t)=100\sin(2\pi 50t) + 100e^{\frac{-t}{0.04}}$
- $I_3(t)=100\sin(2\pi 50t) + 100e^{\frac{-t}{0.06}}$

Fig. 4(a)–(c) show the time-domain response of the proposed filtering algorithm for different current signals. It can be deduced from Fig. 4 that the proposed filter exhibits a fast convergence to the desired value. For a time constant of three cycles (0.06 sec), the proposed filter converges to the final value very quickly.

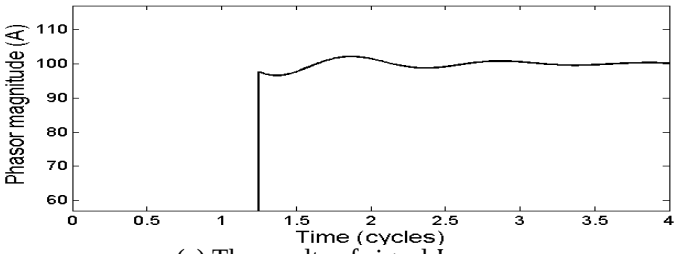
To provide a clear view of the performance of the proposed filter, two performance indices PRMSE and PPE are used; the percentage root mean square error (PRMSE) index determines the average error in one cycle, and the percentage peak error (PPE) index determines the maximum output error. These two indices are calculated as follows [1]:

$$\text{PRMSE}=\frac{\sqrt{\sum_{n=k}^{k+N-1}\frac{(\text{Filter output}-\text{Desired value})^2}{N}}}{\text{Desired value}}\times 100\ \% \quad (25)$$

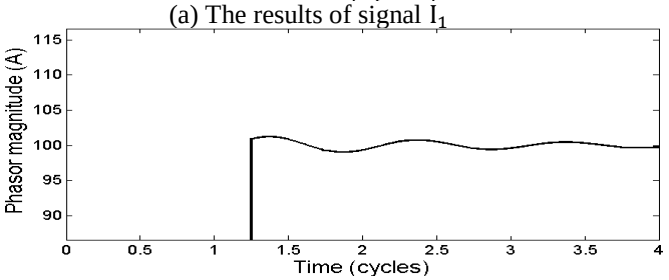
$$\text{PPE}=\frac{\text{Max}|\text{Filter output}-\text{Desired value}|}{\text{Desired value}}\times 100\% \quad (26)$$

Where: k is the beginning index, for example, $k = N+\frac{N}{4}$ for the proposed filter.

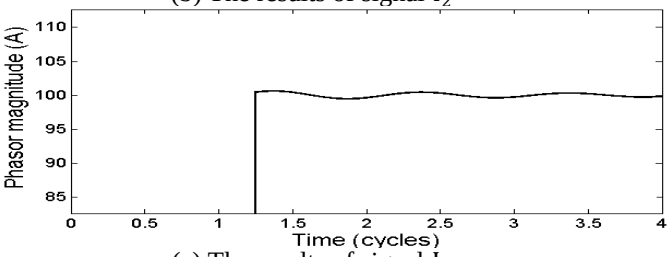
Table 2 depicts the performance indices of the proposed algorithm for the previous simulated current test signals. From Table 2, it can be concluded that the proposed filter algorithm has a minor error and perfect performance.



(a) The results of signal I_1



(b) The results of signal I_2



(c) The results of signal I_3

Fig. 4 Fundamental phasor magnitude responses of proposed filtering algorithm for some test signals with varied time constants

Table 2
Error analysis of proposed filter algorithm for some test signals with varied time constants

Error Index	Tested signals magnitudes estimation (sinusoidal component and DC offset)		
	$I_1(t)$	$I_2(t)$	$I_3(t)$
PRMSE (%)	1.94	0.76	0.40
PPE (%)	3.43	1.24	0.63

Case II: Distorted test signals

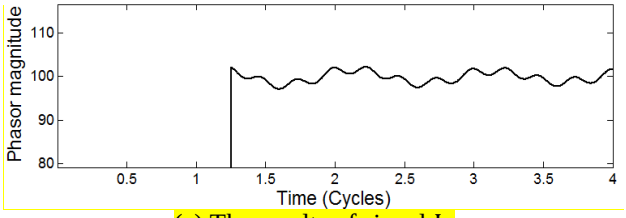
The effectiveness of the proposed algorithm is validated by investigating its performance for two other test signals. Each signal contains fundamental component, DC component, decaying DC component (which has sub-harmonics), and integer harmonics up to 6th order are considered. Also, a random noise is added to one of the test signals $I_5(t)$ to demonstrate the noise immunity effects of proposed algorithm. The noise is generated via the "randn" function in MATLAB. The ratio between maximum noise and the magnitude of fundamental frequency is about 10%.

- $I_4(t) = 50 + \sum_{r=1}^{6}\frac{100}{r}\sin[r\omega t] + 50e^{\frac{-t}{0.06}}$
- $I_5(t) = 50 + \sum_{r=1}^{6}\frac{100}{r}\sin[r\omega t] + 50e^{\frac{-t}{0.06}} + \text{noise}$

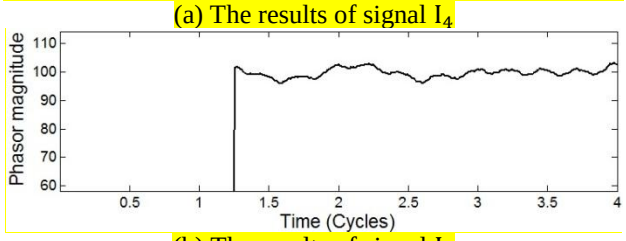
Fig. 5(a)-(b) depict the filtered results of the fundamental frequency component magnitude of I_4 and I_5 respectively. Notably, when the measurement

BUPT

noise is considered, the proposed algorithm still has the same performance. The PRMSE index for I_4, I_5 are 1.97, 1.98 respectively, while the PPE index for I_4, I_5 are 3.5, 3.6 respectively. Actually, the maximum fluctuation range is still bounded in an acceptable range and thus it can be deduced that the proposed filter gives accepted results even in worst cases.



(a) The results of signal I_4



(b) The results of signal I_5

Fig. 5 Fundamental phasor magnitude responses of proposed filtering algorithm for some distorted test signals

5.2 Performance Analysis using Simulated Transmission System

In this part, the performance of the proposed filter is evaluated using a tested transmission line simulated by ATP program. Figure 6 shows the simulated 60 km transmission system, its parameters are fully listed in Appendix B [13].

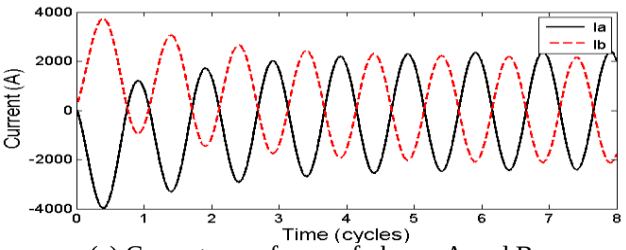
The proposed filter is extensively tested for all fault types (symmetrical and unsymmetrical faults) during different fault locations and fault inception angles for creating a wide range of DC decaying component in current signals. In fact, the proposed filter gives excellent performance for all tested cases.

One of the critical tested cases, which gives high positive and negative values of the exponential component, is illustrated here as an example to ensure the performance of the proposed filter. A-B phase fault is created at distance of 40 km from bus A with fault resistance value equals to 1Ω. The fault inception angle is set at 0° with respect to phase-A voltage waveform of bus A to produce a large decaying DC component. The simulation graphs, shown in Figure 7, are plotted at the instant of fault occurrence. Figure 7 (a) depicts the waveform of the faulted current signals, while the estimated fundamental phasors magnitudes are shown in Fig 7 (b) and (c). Fig 7 (d) depicts the angle difference between phase-A and phase-B current waveforms for proposed filtering algorithm.

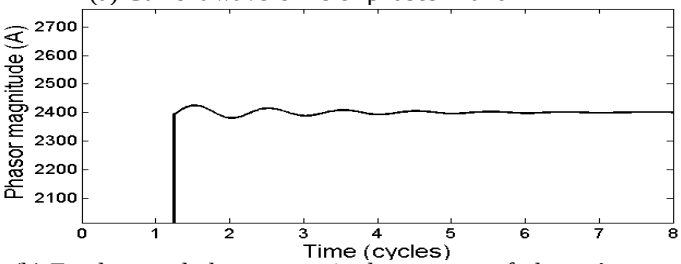
It can be concluded from these figures that the proposed filter has superior magnitude response and phase angle response for such current singles which recover rapidly to the desired value without fluctuations. Moreover, the values of the index PRMSE (%) of the estimated phasors magnitudes of phases A and B current signals are 0.65, 0.74, respectively, while the values of the index PPE (%) of phases A and B are 1.04, 1.21, respectively. These performance indices ensure the effectiveness of the proposed algorithm in filtering fault current signals.



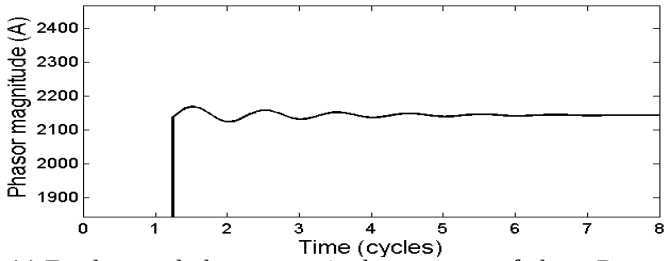
Fig. 6 Single line diagram of the simulated transmission system



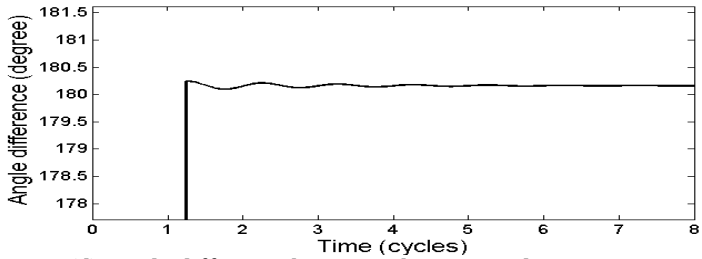
(a) Current waveforms of phases A and B



(b) Fundamental phasor magnitude response of phase-A current



(c) Fundamental phasor magnitude responses of phase-B current



(d) Angle difference between phases A and B

Fig. 7 Current waveforms and the results of proposed filter under A-B fault at 40 km from bus A

BUPT

6. Conclusions

This paper proposed an innovative filtering algorithm for estimating fundamental power system phasors using only one and quarter cycle data window. The comprehensive simulation results assure that the proposed algorithm provides superior rejection capability of the exponentially decaying DC offsets and performs very efficiently in computing the root mean square (r.m.s) and the angle of any electrical signal. The proposed filter, which is designed in discrete formula, can be easily applied to any digital protective relays.

Most power system faults create DC decaying components in current signals, and high-frequency oscillations in voltage signals. Thus, the proposed filtering algorithm is more suitable for filtering current signals. Meanwhile, the proposed filter can also be used in conjunction with an appropriate analog low pass filter to filter out the high-frequency oscillations and precisely estimate the fundamental phasors of voltage signals.

APPENDIX A

The proof of $F1 = M \times A_1 \sin(\Phi_1)$ can be carried out using the following procedures.

The continuous signal x(t) expressed in Equation (1) can be written as follows:

$$x(t) = x_0 + x_1 + \sum_{r=1}^{\infty} x_{2r} + \sum_{r=1}^{\infty} x_{10r-5} \quad \text{(A-1)}$$

Where: $A_1\sin(\omega t + \Phi_1) = x_1$, $A_{2r}\sin(2r\omega t + \Phi_{2r}) = x_{2r}$, $A_0 = x_0$, $A_{10r-5}\sin[(10r-5)\omega t + \Phi_{(10r-5)}] = x_{10r-5}$, and r =1,2,3,4,5,6,…, ∞ .

Also, the Equation (2) can be written as follows:

$$F1 = f_0 + f_1 + \sum_{r=1}^{\infty} f_{2r} + \sum_{r=1}^{\infty} f_{10r-5} \quad \text{(A-2)}$$

Putting *i*= (0), (1), (2r), or $(10r-5)$.

$$\text{Then, } f_i = \int_0^{T/4} x_i dt - \int_{T/4}^{13T/20} x_i dt + \int_{17T/20}^{T} x_i dt + \int_0^{3T/20} x_i dt - \int_{7T/20}^{3T/4} x_i dt + \int_{3T/4}^{T} x_i dt + \int_0^{T/5} x_i dt - \int_{2T/5}^{3T/5} x_i dt + \int_{4T/5}^{T} x_i dt + \int_0^{T/10} x_i dt - \int_{3T/10}^{7T/10} x_i dt + \int_{9T/10}^{T} x_i dt \quad \text{(A-3)}$$

By using Equation (A-3), the value of f_0 can be obtained as follows (*i* =0): $f_0 =$

$$A_0[t]_0^{\frac{T}{4}} - A_0[t]_{\frac{T}{4}}^{\frac{13T}{20}} + A_0[t]_{\frac{17T}{20}}^{T} + A_0[t]_0^{\frac{3T}{20}} - A_0[t]_{7T/20}^{3T/4} + A_0[t]_{3T/4}^{T} + A_0[t]_0^{T/5} - A_0[t]_{2T/5}^{3T/5} + A_0[t]_{4T/5}^{T} + A_0[t]_0^{T/10} - A_0[t]_{3T/10}^{7T/10} + A_0[t]_{9T/10}^{T}$$

Thus, $f_0 = 0$

The value of f_1 can be obtained by using Equation (A-3) as follows (*i* =1): $f_1 =$

$$\frac{A_1}{\omega}[-\cos(\omega t + \Phi_1)]_0^{\frac{T}{4}} - \frac{A_1}{\omega}[-\cos(\omega t + \Phi_1)]_{T/4}^{13T/20} + \frac{A_1}{\omega}[-\cos(\omega t + \Phi_1)]_{17T/20}^{T} + \frac{A_1}{\omega}[-\cos(\omega t + \Phi_1)]_0^{3T/20} - \frac{A_1}{\omega}[-\cos(\omega t + \Phi_1)]_{7T/20}^{3T/4} + \frac{A_1}{\omega}[-\cos(\omega t + \Phi_1)]_{3T/4}^{T} + \frac{A_1}{\omega}[-\cos(\omega t + \Phi_1)]_0^{T/5} - \frac{A_1}{\omega}[-\cos(\omega t + \Phi_1)]_{2T/5}^{3T/5} + \frac{A_1}{\omega}[-\cos(\omega t + \Phi_1)]_{4T/5}^{T} + \frac{A_1}{\omega}[-\cos(\omega t + \Phi_1)]_0^{T/10} - \frac{A_1}{\omega}[-\cos(\omega t + \Phi_1)]_{3T/10}^{7T/10} + \frac{A_1}{\omega}[-\cos(\omega t + \Phi_1)]_{9T/10}^{T}$$

After some algebraic manipulations, it yields:

$$f_1 = \frac{4\left[1+\sin\left(\omega\times\frac{3T}{20}\right)+\sin\left(\omega\times\frac{T}{5}\right)+\sin\left(\omega\times\frac{T}{10}\right)\right]}{\omega} \times A_1 \sin(\Phi_1)$$

The value of f_{2r} can be obtained by using Equation (A-3) as follows (*i* =2r): $f_{2r} =$

$$\frac{A_{2r}}{2r\omega}[-\cos(2r\omega t + \Phi_{2r})]_0^{\frac{T}{4}} - \frac{A_{2r}}{2r\omega}[-\cos(2r\omega t + \Phi_{2r})]_{T/4}^{13T/20} + \frac{A_{2r}}{2r\omega}[-\cos(2r\omega t + \Phi_{2r})]_{17T/20}^{T} + \frac{A_{2r}}{2r\omega}[-\cos(2r\omega t + \Phi_{2r})]_0^{3T/20} - \frac{A_{2r}}{2r\omega}[-\cos(2r\omega t + \Phi_{2r})]_{7T/20}^{3T/4} + \frac{A_{2r}}{2r\omega}[-\cos(2r\omega t + \Phi_{2r})]_{3T/4}^{T} + \frac{A_{2r}}{2r\omega}[-\cos(2r\omega t + \Phi_{2r})]_0^{T/5} - \frac{A_{2r}}{2r\omega}[-\cos(2r\omega t + \Phi_{2r})]_{2T/5}^{3T/5} + \frac{A_{2r}}{2r\omega}[-\cos(2r\omega t + \Phi_{2r})]_{4T/5}^{T} + \frac{A_{2r}}{2r\omega}[-\cos(2r\omega t + \Phi_{2r})]_0^{T/10} - \frac{A_{2r}}{2r\omega}[-\cos(2r\omega t + \Phi_{2r})]_{3T/10}^{7T/10} + \frac{A_{2r}}{2r\omega}[-\cos(2r\omega t + \Phi_{2r})]_{9T/10}^{T}$$

After some algebraic manipulations, it yields:

$$f_{2r} = 0$$

The value of f_{10r-5} can be obtained by using Equation (A-3) for $i = 5b$. (where $b = 2r-1$).

$f_{5b} =$

$$\frac{A_{5b}}{5b\omega}[-\cos(5b\omega t + \Phi_{5b})]_0^{\frac{T}{4}} - \frac{A_{5b}}{5b\omega}[-\cos(5b\omega t + \Phi_{5b})]_{\frac{T}{4}}^{\frac{13T}{20}} + \frac{A_{5b}}{5b\omega}[-\cos(5b\omega t + \Phi_{5b})]_{17T/20}^{T} + \frac{A_{5b}}{5b\omega}[-\cos(5b\omega t + \Phi_{5b})]_0^{3T/20} - \frac{A_{5b}}{5b\omega}[-\cos(5b\omega t + \Phi_{5b})]_{7T/20}^{3T/4} + \frac{A_{5b}}{5b\omega}[-\cos(5b\omega t + \Phi_{5b})]_{3T/4}^{T} + \frac{A_{5b}}{5b\omega}[-\cos(5b\omega t + \Phi_{5b})]_0^{T/5} - \frac{A_{5b}}{5b\omega}[-\cos(5b\omega t + \Phi_{5b})]_{2T/5}^{3T/5} + \frac{A_{5b}}{5b\omega}[-\cos(5b\omega t + \Phi_{5b})]_{4T/5}^{T} + \frac{A_{5b}}{5b\omega}[-\cos(5b\omega t + \Phi_{5b})]_0^{T/10} - \frac{A_{5b}}{5b\omega}[-\cos(5b\omega t + \Phi_{5b})]_{3T/10}^{7T/10} + \frac{A_{5b}}{5b\omega}[-\cos(5b\omega t + \Phi_{5b})]_{9T/10}^{T}$$

After some algebraic manipulations, it yields:

$$f_{5b} = f_{10r-5} = 0$$

Finally, it can be concluded that the value of

BUPT

$f_i = 0$ for $i = 0$, (i =2r), or ($i = 5 \times (2r - 1)$). Hence, F1 = f_1

APPENDIX B

The parameters of the simulated power system are shown as follows:

Equivalent source impedance:
Source A:
Z_{A1}=0.238 + j 12.4 (Ω), Z_{A0}=2.738 + j 21.9 (Ω) , φ=0°
Source B:
Z_{B1}=0.238+j13.2 (Ω), Z_{B0}=0.83 + j 10.8 (Ω), φ=-10°

Transmission line parameters:
R_1=0.0196 (Ω/km),R_0=0.2079 (Ω/km)
L_1=1.011 (mH/km),L_0=2.552 (mH/km)
C_1=14.167 (nF/km),C_0=7.668 (nF/km)

REFERENCES

[1] Chi-Shan Yu , Yi-Sheng Huang ,and Joe-Air Jiang: *A Full- and Half-Cycle DFT- based Technique for Fault Current Filtering*. In: Proceedings of the IEEE Industrial Technology Conference, March 2010, p. 859-864.

[2] Sun-Li Yu and Jyh Cherng Gu: *Removal of Decaying DC in Current and Voltage Signals Using a Modified Fourier Filter Algorithm*. In: IEEE Transactions on Power Delivery, July (2001), Vol. 16, No. 3, pp. 372 - 379.

[3] J. Yang and C. Liu: *Complete elimination of DC offset in current signals for relaying applications*, In: Proceedings of the IEEE PES Society Winter Meeting, Feb. 2000, Vol. 3, p. 1933-1938

[4] J.F. Miñambres Argüelles, M.A. Zorrozua Arrieta, B. Larrea Jaurrieta, and M.Sanchez Benito: *A new method for decaying DC offset removal for digital protective relays*. In: Electric Power Systems Research, (2006), Vol. 76, p. 194-199.

[5] Kamel N.A. Al-Tallaq, H.D. Al-Sharai, M.E. El-Hawary: *Online algorithm for removal of decaying DC-offset from fault currents*. In: Electric Power Systems Research, (2011), Vol. 81, p. 1627-1629.

[6] Sang-Hee Kang, Dong-Gyu Lee, Soon-Ryul Nam, P.A. Crossley, Yong-Cheol Kang: *Fourier transform-based modified phasor estimation method immune to the effect of the DC offsets*. In: IEEE Transactions on Power Delivery, (2009), Vol. 24, p. 1104-1111.

[7] H.B. El Refaie, A.I. Megahed: *A novel technique to eliminate the effect of decaying DC component on DFT based phasor estimation*. In: Proceedings of the IEEE Power and Energy Society General Meeting, 2010, p. 1-8.

[8] D.K. Ibrahim, M.E. Rezk, E.E. Abo El-Zahab: *Improving distance protection performance at zone1 using new adaptive tripping time scheme*. In: Proceedings of the IEEE International Energy Conference (ENERGYCON), 2014, p. 528-535.

[9] T.S. Sidhu, X. Zhang, V. Balamourougan. *A new half-cycle phasor estimation algorithm*, In: IEEE Transactions on Power Delivery, (2005), Vol. 20, p. 1299 -1305.

[10] Siemens AG, Energy Sector, User manual SIPROTEC 5 device family, Document version: C53000-G5040-C010-4, [Online]. Available: http://www.siprotec.com

[11] H.J. Altuve, I. Diaz, E. Vazquez: *Fourier and Walsh digital filtering algorithms for distance protection*. In IEEE Transactions on Power Systems, (1996), Vol. 11, p. 423-428.

[12] A. Abdollahi, Peng Zhang: *Precise removal of decaying DC in DFT algorithm for power system measurement*. In: Proceedings of IEEE Power and Energy Society General Meeting Conference, 2012, p. 1-7.

[13] Ching-Shan Chen, Chih-Wen Liu, Joe-Air Jiang: *Application of combined adaptive Fourier filtering technique and fault detector to fast distance protection*. In: IEEE Transactions on Power Delivery, (2006), Vol. 21, p. 619-626.

BUPT